

# Modeling Storm Surge in a Small Tidal Two-Inlet System

Matthew Reffitt<sup>1</sup>; Mara M. Orescanin<sup>2</sup>; Chris Massey<sup>3</sup>; Britt Raubenheimer, A.M.ASCE<sup>4</sup>; Robert E. Jensen<sup>5</sup>; and Steve Elgar<sup>6</sup>

**Abstract:** Model simulations using a depth-averaged ocean circulation model (ADCIRC) two-way coupled with a wave model (STWAVE) through the Coastal Storm Modeling System Coupling Framework (CSTORM-MS) are compared with observations made in the shallow, two-inlet tidal Katama Bay system on the Atlantic coast of Martha's Vineyard, Massachusetts, during Hurricane Irene. The CSTORM-MS framework integrates high-resolution bathymetric grids of this system with the North Atlantic Coast Comprehensive Study (NACCS) performed by the United States Army Corps of Engineers. The effects of bathymetric resolution and wave-flow coupling on the accuracy of modeled storm surge were investigated by comparing observations with the high bathymetric resolution, coupled model (CSTORM), a high-resolution uncoupled ADCIRC model, and a low bathymetric resolution, coupled model (NACCS). During the peak storm surge period, the coupled model using high-spatial resolution bathymetry reduced error in the study area by over 30% compared with the lower-resolution NACCS model, and by 16% compared with the high-resolution, uncoupled ADCIRC model. In addition, the high-resolution models indicate alongshore flows with magnitudes over 2.0 m/s along the southern coast of Martha's Vineyard, and a net northward circulation through Katama Bay and Edgartown Channel, which are not apparent in the lower-resolution simulations. Contrary to prior research suggesting small, if any setup in the Katama Bay system from wave forcing, in the extreme wave forcing event discussed here, the northward flux through Katama Inlet on the south side of the bay does not exit completely through Edgartown Channel on the north side of Katama Bay. Thus, the drainage path is not adequate to prevent increased water elevation in the bay, resulting in a setup within Katama Bay during the peak surge event, highlighting the need for adequate model resolution for local storm surge predictions. DOI: 10.1061/(ASCE)WW.1943-5460.0000606. © 2020 American Society of Civil Engineers.

## Introduction

### Background

Storm surge, or the increase in water level associated with a meteorological event, often accounts for a significant percentage of the property damage caused by hurricanes (Neumann et al. 2015). In addition, coastal flooding associated with storm surge can create a hazard to residents that often is a major contributor to high death tolls (Blake et al. 2007). To provide adequate warning to prevent the loss of life and property, storm surge must be predicted accurately. However, storm surge in spatially small systems with complex bathymetry, such as tidal inlets, can be difficult to predict with regional-scale storm-surge forecast modeling systems that necessitate coarse spatial resolution (Yin et al. 2016). For example, storm surge in inland areas of the US Gulf Coast was not predicted accurately with low-resolution models during Hurricane Ike (Kerr et al. 2013), nor was storm surge predicted accurately for barrier

island systems along the US East Coast (Lawler et al. 2016; Bennett et al. 2018).

Coupling high-resolution storm-surge models with nearshore wave models is an active research field (Dietrich et al. 2012; Orton et al. 2012; Sun et al. 2013; Mao and Xia 2018; Kang and Xia 2020) motivated by observations of wave effects on water levels in back lagoons and currents within tidal inlets (Bertin et al. 2009; Malhadas et al. 2009; Dodet et al. 2013; Orescanin et al. 2014). There are several examples of such modeling systems, including the coupling of the unstructured version of the Simulating Waves Nearshore (SWAN) and the Advanced Circulation (ADCIRC) models (Dietrich et al. 2012), coupling of Delft3D and SWAN (Bennett et al. 2018), the Coupled-Ocean-Atmosphere-Wave-Sediment Transport (COAWST) model (Kumar et al. 2011), and FVCOM/SWAVE (Chen et al. 2013). Neglecting small-scale bathymetric features, such as tidal inlets or shoals, and the associated hydrodynamics, can lead to underprediction of storm surge relative to simulations that include high-resolution bathymetry and small-scale processes (Orton et al. 2012; Sun et al. 2013).

The Steady-State Spectral Wave Model (STWAVE) accounts for both wave diffraction and reflection (Gonçalves et al. 2015), which may be important near the complex bathymetry of tidal inlet systems where observations show large spatial gradients of currents, waves, and bathymetry. Using the Coastal Storm Modeling System Coupling Framework (CSTORM-MS) (Massey et al. 2011b), STWAVE and ADCIRC coupled modeling of storm surge is skillful on large spatial scales (Bryant and Jensen 2017). Less research has been conducted at the higher resolutions needed to resolve most inlet and small bay systems that are common along barrier island coastlines. Model domain sizes that are not sufficiently large underestimate storm surge (Blain et al. 1994); therefore, nested model domains are an option to increase resolution in areas of interest while minimizing computational cost.

<sup>1</sup>Dept. of Oceanography, Naval Postgraduate School, Monterey, CA 93943.

<sup>2</sup>Dept. of Oceanography, Naval Postgraduate School, Monterey, CA 93943 (corresponding author). ORCID: <https://orcid.org/0000-0002-0865-2738>. Email: [msoresca@nps.edu](mailto:msoresca@nps.edu)

<sup>3</sup>US Army, Engineering Research and Development Center, Coastal Hydraulics Laboratory, Vicksburg, MS 39180-6199.

<sup>4</sup>Woods Hole Oceanographic Institution, Woods Hole, MA 02543.

<sup>5</sup>US Army, Engineering Research and Development Center, Coastal Hydraulics Laboratory, Vicksburg, MS 39180-6199.

<sup>6</sup>Woods Hole Oceanographic Institution, Woods Hole, MA 02543.

Note. This manuscript was submitted on February 3, 2020; approved on June 10, 2020; published online on September 10, 2020. Discussion period open until February 10, 2021; separate discussions must be submitted for individual papers. This paper is part of the *Journal of Waterway, Port, Coastal, and Ocean Engineering*, © ASCE, ISSN 0733-950X.

## Study Parameters

The focus here is the Katama Inlet system, Martha's Vineyard, Massachusetts (Fig. 1), during Hurricane Irene. Pressure sensors were deployed in the Bay from Katama Inlet in the south to Edgartown Channel in the north in early August, 2011, and remained in place until after Hurricane Irene (Fig. 1 and Orescanin et al. 2014). The observations are used here to examine the skill of coupled wave and circulation models with different spatial resolutions.

Irene (Atlantic storm number 09) passed approximately 550 km to the west on 28 August, 2011. Significant wave heights measured at the closest offshore NOAA buoy (Number 44097) reached a peak of 14.7 m at 12:38 EDT on August 28, much higher than the typical non-storm value of 1.0 m. Martha's Vineyard Coastal Observatory (MVCO) recorded significant wave heights over 5 m in 12-m water depth [Fig. 2(a)]. Maximum sustained winds at the NOAA buoy at Buzzards Bay located 55 km to the west of the research area and at MVCO [Fig. 2(b)] at the time of the closest point of approach were approximately 25 m/s. Storm surge associated with Irene propagated northward through the research area and was 0.7 m at the southernmost observation sensor in Katama Bay [Station 03 in Fig. 1, and the observed time series in Fig. 2(e)] on August 28 at 14:45 EDT.

Katama Bay and the surrounding Atlantic Ocean (including Wasque Shoals, south of Katama Inlet) is an area of complex bathymetry that includes the migrating Katama Inlet that, when open, connects the southern part of the bay with the Atlantic Ocean (Fig. 1). Katama Inlet last opened during a nor'easter storm in 2007 and slowly migrated 1.5 km to the east until it closed in 2015, producing complicated, evolving ebb and flood shoals. These shoals and Norton Point are comprised of medium sand. Katama Bay is connected to Vineyard Sound in the north by the continuously open Edgartown Channel (Fig. 1). Thus, when Katama Inlet is open, this site is a double inlet system. The M2 tide at Edgartown Channel in Vineyard

Sound is approximately 3 h out of phase (delayed) with the Atlantic M2 tides at Katama Inlet. This phase difference results in strong tidal flows in the inlets and the bay. However, under normal conditions, subtidal changes in the bay sea level are small because water can flow out of the inlets (Orescanin et al. 2014). In addition, there is no significant freshwater input to the system that would distort the tidally driven flows.

The complex bathymetry covers a relatively small area and, thus, is an ideal location to study the effects of spatial resolution on models for storm surge. Previous modeling in this area focused on wave-current interaction (Hopkins et al. 2016), sediment transport processes (Hopkins et al. 2017), and the effect of temporally varying inlet geometry on bay circulation (Orescanin et al. 2016). Numerical results suggest that high-spatial-resolution bathymetry, both within Katama Bay and in the Atlantic Ocean offshore of Katama Inlet, combined with accurate wave models are critical to simulate the hydrodynamics of the system.

Here, the importance of spatial resolution and wave forcing to simulations of storm surge through small coastal bays and inlets is investigated. Specifically, STWAVE and ADCIRC are dynamically two-way coupled using the CSTORM coupler, and the peak storm surge and flow predictions are compared with the predictions of uncoupled or lower-resolution modeling systems. Large domain ADCIRC meshes and STWAVE grids created by the United States Army Corps of Engineers for the North Atlantic Coast Comprehensive Study (NACCS) (Cialone et al. 2015, 2017) are utilized and merged with higher-resolution grids.

## CSTORM Numerical Models

The Coastal Storm Modeling System (CSTORM-MS) is a system of numerical models used to simulate coastal storm waves and

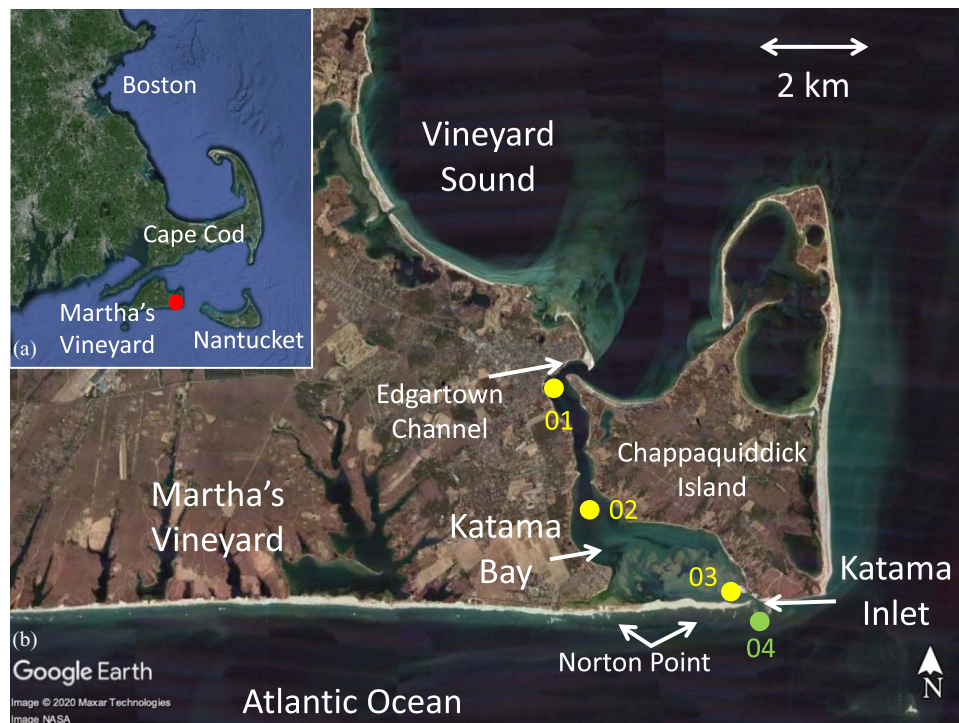


**Fig. 1.** Location of (a) Martha's Vineyard, Massachusetts, with the Katama system inside the red circle; and (b) the south-eastern part of Martha's Vineyard, showing Katama Bay, with Edgartown Channel to the north and Katama Inlet to the south. The yellow circles are sensor locations, and the green circle (04) is located on the ebb shoal where model results are compared with each other. (Map © 2020 Google, image © 2020 Maxar Technologies, image NASA.)

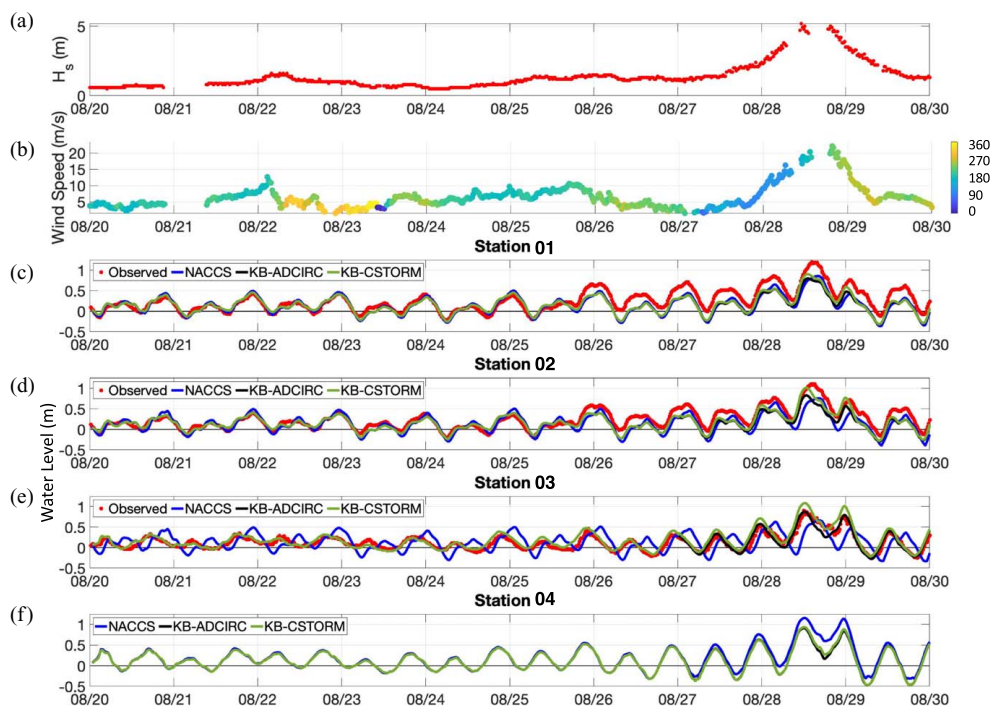


**Fig. 2.** Time series of waves, wind speed, and direction, and water level for the Katama Bay system: (a) significant wave height ( $H_s$ ) and (b) wind speed (colored by direction, scale on the right) for MVC0 (12-m depth), and water-surface elevation for (c) Station 01; (d) Station 02; (e) Station 03; and (f) Station 04 versus time during Hurricane Irene, which had a maximum impact in this area midday on 28 August. The curves are for observations (red), NACCS (blue), KB-ADCIRC (black), and KB-CSTORM (green), where KB refers to the high resolution Katama Bay mesh. Observations were not obtained at Station 04.

water levels, as well as a comprehensive methodology of how those models are applied to provide accurate inputs for assessing risk to coastal communities. The CSTORM-MS makes use of nonlinear physics-based models with higher-order-accurate numerical discretization methods and resolutions. The numerical models used within the CSTORM modeling system for the NACCS consisted of the deep-water Wave Model (WAM) for producing offshore wave boundary conditions for use with the nearshore STWAVE model. The ADCIRC model was used to simulate two-dimensional depth-integrated surge and circulation responses to the storm conditions. The STWAVE model was used to provide the nearshore wave conditions, including local wind-generated waves. The CSTORM coupling framework (Massey et al. 2011b) was used to tightly two-way couple the ADCIRC and STWAVE models to allow for dynamic interactions between the surge, circulation, and waves, resulting in improved modeling results.

### Wind and Pressure Fields

The wind and pressure fields used for the Hurricane Irene simulations were produced by Oceanweather, Inc. (OWI 2015) and are the same winds and pressures used and documented as part of the NACCS (Cialone et al. 2015). Two levels of wind and pressure fields were used (Fig. 3). The first level included a larger domain covering the western Atlantic from  $99.0^\circ$  to  $60.0^\circ$  west longitude and from  $7.500^\circ$  to  $46.125^\circ$  north latitude using a  $0.125^\circ$  grid resolution [larger grid, Fig. 3(a)]. The second level covered an area from  $78.00^\circ$  to  $72.00^\circ$  west longitude and from  $34.00^\circ$  to  $42.05^\circ$  north latitude using a grid resolution of  $0.05^\circ$  (smaller grid, Fig. 3(a)). The wind and pressure field records were sampled every 15 min and covered the period from 08/20/2011 0 h UTC to 08/30/2011 0 h UTC. The study area [red X, Fig. 3(a)] was

located in the larger wind and pressure domain with a gridded resolution of  $0.125^\circ$ .

Several National Data Buoy Center (NDBC) and one National Estuarine Research Reserve System (NERRS) locations recorded wind speeds and directions during Hurricane Irene near the study area. Of those, three representative sites were selected to compare wind speeds and directions, and two sites were selected to compare wave statistics [diamonds in Fig. 3(b)]. The selected NDBC sites for wind comparisons are NTKM3 [“C” in Fig. 3(b)] on Nantucket Island, Massachusetts [Figs. 4(a and b)], and Station 44020 [“B” in Fig. 3(b)] in Nantucket Sound (Fig. 5). The measured and modeled wind speeds are similar (Figs. 4 and 5), with the modeled values for peak wind speeds slightly overpredicted by approximately 5 m/s at Station NTKM3 and the Waquoit Bay Reserve NERRS [Figs. 4(a and c)]. The wind directions at these locations [Figs. 4(b and d) and 5(f)] also compare well, although there is an approximately  $30^\circ$  shift in the wind directions at the NERRS location. Considering the  $0.125^\circ$  resolution of the modeled winds, the simulated values are considered to represent the storm well in this small bay.

### WAM Wave Model

The deep-water wave model used to generate the offshore wave estimates for the NACCS and, consequently for this study, is the third-generation wave model WAM (Komen et al. 1994). WAM is similar to other third-generation wave models like WaveWatch III (Tolman 2014) or SWAN (SWAN Team 2017). WAM makes no a priori assumptions governing the spectral shape of the waves, and the source term solution is formulated to the wave model’s frequency/directional resolution. WAM was developed by a consortium of wave theoreticians and modelers over a 10-year period and is used by the European Center for Medium-Range



**Fig. 3.** (a) Map showing the outline of the ADCIRC model domain boundaries in dark blue and the boundaries of the two wind and pressure field domains in red. A red X demarks the study area. (b) Map showing a more detailed view of the project area, with the ADCIRC model domain boundaries in dark blue and the black gridded lines showing the grid cells for the Level 1 wind and pressure fields. Winds were observed at the four locations marked with yellow diamonds, with waves observed at yellow diamonds A and B. The red X demarks the study area.

Weather Forecasts researchers and in the private sector. The accuracy of the WAM model's results is dictated by the accuracy in the bathymetric grid and wind forcing data used in the simulations.

The WAM results are used to provide spectral energy boundary conditions to the nearshore STWAVE model. This splitting up of waves between deep water and nearshore allows for a more computationally efficient workflow for CSTORM and the use of wave models specifically designed for deep water and shallow water, respectively. Since the WAM model uses a coarser spatial resolution than STWAVE and uses integer values for water depths, the WAM model is insensitive to changes in the geometry of the nearshore areas or water depth changes on the order of a meter or two. The STWAVE model, as most other nearshore wave models, is comparatively more computationally expensive than a 2D circulation model such as ADCIRC and, in general, requires between 4 and 18 times the computational effort. As such, reducing the simulation region of the nearshore wave models, without significantly compromising nearshore results for waves and water levels, is desirable. Using the WAM model results to force the boundary of the STWAVE model allows swell propagating from far offshore to be included in the simulations, while reducing the computational time required by STWAVE. The WAM model setup used in this study is exactly the same as that used in the NACCS (Cialone

et al. 2015; Jensen et al. 2016). These reports provide significant details of the WAM model setup and validation results applied to several historical tropical and extra-tropical events, including Hurricane Irene. A sample of the WAM model result for Hurricane Irene is compared with measurement data at two NDBC buoys located near the study area, Station 44020 (Fig. 5) and Station 44097 (Fig. 6). In the more open water areas around Buoy 44097, the WAM results represent the significant wave heights, peak, and mean periods very well. However, Buoy 44020 is located near Nantucket and Martha's Vineyard islands, including the Katama Bay system, and the WAM model resolution is not designed specifically to capture them. This can be seen in the time series (Fig. 5), where the periods from the model indicate swells, and the measurements indicate wind seas. Nevertheless, the model does well at reproducing the significant wave heights.

### Steady-State Spectral Wave Model

#### Model Description

STWAVE is a model developed by the United States Army Corps of Engineers to estimate wind-wave growth and nearshore wave transformation, including shoaling, breaking, diffraction, and refraction. STWAVE is a finite-difference, phase-averaged spectral model that solves the wave action balance equation on a Cartesian, rectangular grid (Massey et al. 2011a). STWAVE is run in full-plane mode, which allows wave generation from all 360° and thus is better suited than half-plane mode for modeling waves during a hurricane. The steady-state STWAVE model operates under the assumption that the duration of meteorological forcing is not a limiting factor in the generation of wind waves over the domain.

#### Model Setup and Domain

Two STWAVE grids are used here (Fig. 7). A larger grid covering the southern Massachusetts (SMA) area developed for the North Atlantic Coast Comprehensive Study (NACCS) (Bryant and Jensen 2017) with a resolution of 200 × 200 m was used to generate wave spectra for boundary conditions for the smaller 10 × 10-m grid covering Katama Bay. Both grids were oriented at 101.5° (Fig. 7). Both models used 72 angle bands separated by 5° and 30 frequency bands ranging from 0.04 to 0.33 Hz in increments of 0.01 Hz. The SMA grid has an origin ( $x_0, y_0$ ) located at (465,575.3; 4,518,084.4) in the UTM zone 19 coordinate system measured in meters and is made up of 733 cells in the I-direction and 887 cells in the J-direction. The Katama Bay grid has an origin ( $x_0, y_0$ ) located at (381,625.68; 4,577,634.03) in the UTM zone 19 coordinate system measured in meters and is made up of 916 cells in the I-direction and 1,134 cells in the J-direction. Waves on the NACCS SMA grid were forced with output from WAM and the (described previously) Hurricane Irene wind fields. Morphic interpolation (Smith and Smith 2002) of the directional spectra was used along the boundary of both STWAVE grids to supply spectral energy inputs to the models, and both models used wave breaking. Independent STWAVE simulations with a static water elevation were run from August 27 to August 30, 2011, to include the effects of Hurricane Irene, which produced a peak surge in the research area on the afternoon of August 28, 2011. Model time steps, or snaps, were set at every 30 min. Bathymetry values for the SMA grid were interpolated from the NACCS ADCIRC mesh, which combined numerous sources to obtain the most accurate bathymetry possible [see Cialone et al. (2015, 2017) for model development discussion and details].

Bathymetry for the high-resolution Katama Bay (KB) grid was obtained from surveys conducted with GPS- and sonar-equipped small boats combined with a 10-m resolution digital elevation

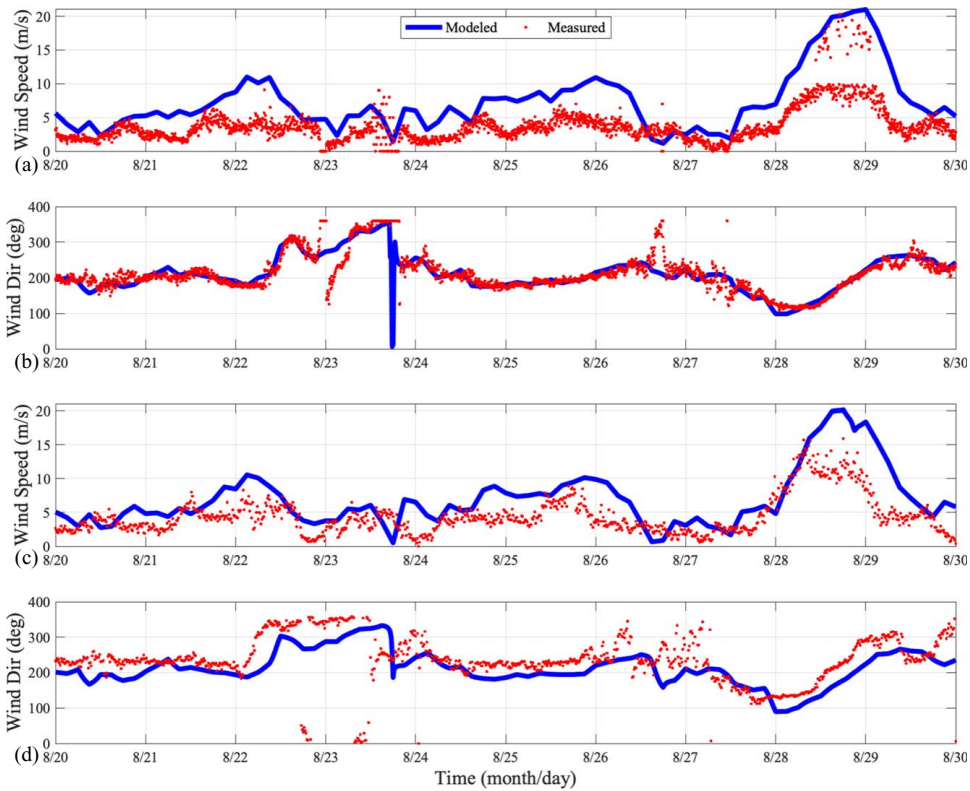


**Fig. 4.** Time series of wind speed and direction at: (a and b) NDBC NTKM3 (Nantucket); and (c and d) NERRS Waquoit Bay Reserve. WAM model inputs used for the NACCS (blue) compared with observations (red). Locations for NTKM3 and Waquoit Bay are shown in Fig. 3(b) (Positions C and D, respectively).

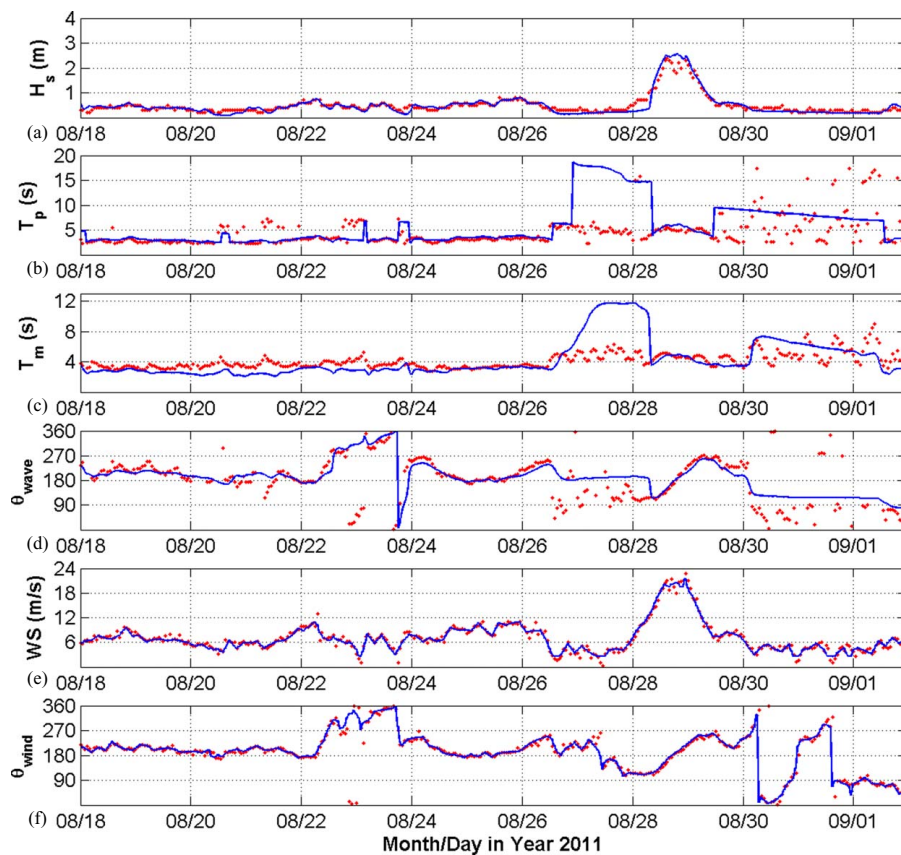


**Fig. 5.** WAM model (blue curves) and NDBC buoy 44020 [red dots, “B” in Fig. 3(b)] versus time: (a) significant wave height; (b) peak period; (c) mean period; (d) wave direction; (e) wind speed; and (f) wind direction.

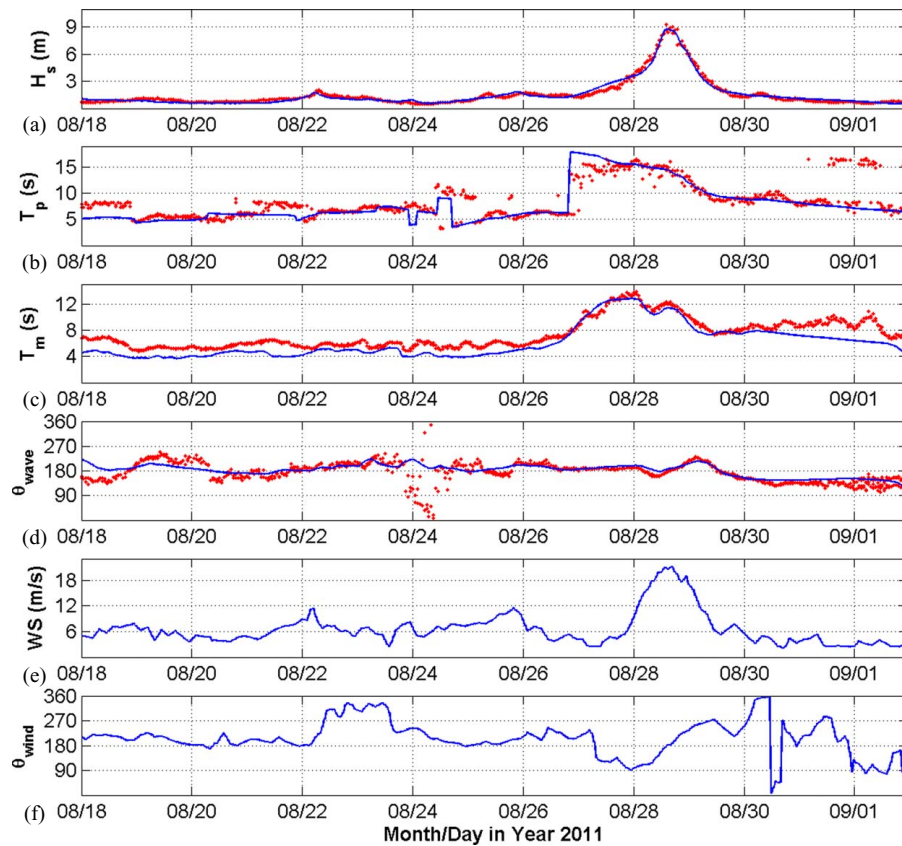


**Fig. 6.** WAM model (blue curves) and NDBC buoy 44097 [red dots, “A” in Fig. 3(b)] versus time: (a) significant wave height; (b) peak period; (c) mean period; (d) wave direction; (e) wind speed; and (f) wind direction.



**Fig. 7.** Southern Massachusetts grid (SMA) (outer green box) and the higher-spatial resolution Katama Bay grid (KB) (inner green box) used for STWAVE.

model produced by NOAA in 2008 (Orescanin et al. 2016). The Katama Bay grid resolves the smaller-scale bathymetric contours of the bay and offshore region, particularly in the vicinity of the inlet and ebb shoal, in contrast to the lower-resolution SMA grid (Fig. 8). Prior to coupling, both nested (Smith and Smith 2002) and un-nested STWAVE model runs conducted for the Hurricane Irene time period using the high-resolution grid were stable. For the large-scale, un-nested-grid case, there were no waves

specified on the southern boundary, with waves generated within the grid using the OWI Hurricane Irene wind field. When using the nested grids, waves on the boundaries of the inner, high-resolution grid were provided by the spectral output from the SMA grid.

### Circulation Model

#### Model Description

The two-dimensional variant of the Advanced Circulation model (ADCIRC) is a depth-averaged model for ocean circulation based on the shallow water equations for conservation of mass and momentum and applies Boussinesq and hydrostatic pressure approximations (Luettich et al. 1992; Westerink et al. 1992). ADCIRC is an unstructured finite-element model, and thus the resolution can be varied across the domain to resolve complex bathymetry and associated processes in areas of interest, while minimizing computational cost by relaxing the resolution in areas where the bathymetry varies more slowly.

#### Model Setup and Domain

Two ADCIRC meshes of differing resolution were used (Fig. 9). The coarser mesh was taken from the NACCS (Cialone et al. 2015, 2017). The finer mesh was developed by merging the Katama Bay mesh (Orescanin et al. 2016) with the NACCS mesh to achieve the resolution required near the coast and within the bay, while simultaneously including the large, basin-scale effects crucial to model storm surge accurately (Blain et al. 1994), here called the KB-ADCIRC mesh. The NACCS mesh treats the southern shoreline of Martha's Vineyard (Figs. 1 and 3) as a hard, no normal-flow boundary [Fig. 9(a)], whereas the high-resolution KB-ADCIRC

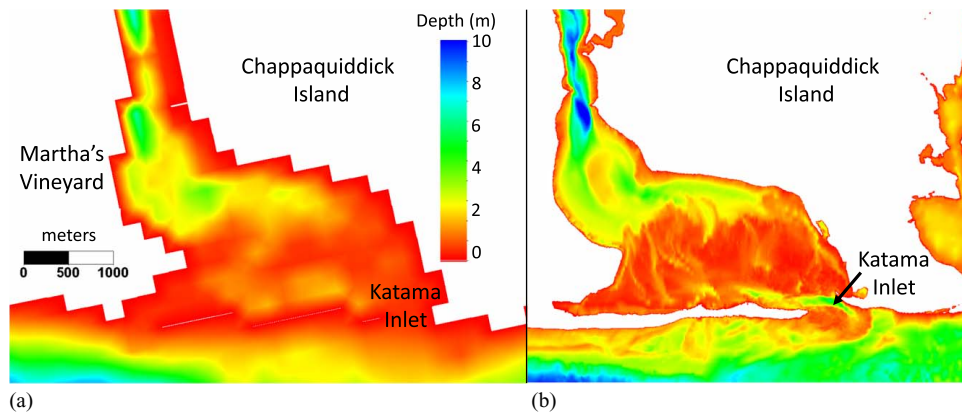


**Fig. 8.** Contours of bathymetry [color and scale bars are in (a)] for (a) the 200 by 200 m coarse SMA STWAVE grid; and (b) the 10 by 10 m fine Katama Bay (KB) STWAVE grid.

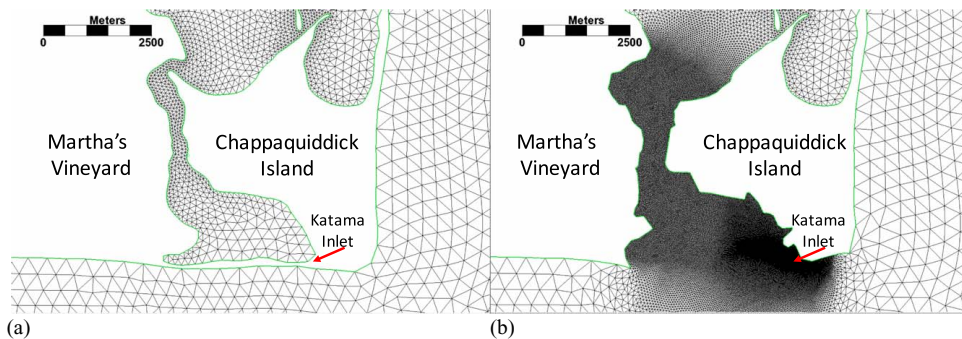


**Fig. 9.** (a) NACCS mesh; and (b) the NACCS and Katama merged ADCIRC mesh.

mesh allows water to overtop the low-elevation Norton Point [Figs. 1 and 3(b)] and to enter Katama Bay through Katama Inlet [Fig. 9(b)]. Tidal forcing was applied to both meshes at the open ocean boundaries near  $60^\circ$  west longitude. Consistent with the STWAVE grids, meteorological forcing was applied from Ocean-weather Hurricane Irene wind and pressure fields. The ADCIRC simulations were run for a period of 24 days consisting of a 14-day tidal spin-up before winds were applied to the domain from August 20 to August 30, 2011. The Courant-limited time step for ADCIRC model runs was 0.5 s. A constant water level adjustment (the *sea surface height above geoid* parameter in ADCIRC) was set to the NACCS value of 0.111 m to represent baroclinic and steric effects not accounted for in the ADCIRC model (Cialone et al. 2015). Values for spatially varying bottom friction, horizontal eddy viscosity, and primitive equation weighting of the continuity equation were the same as those in the NACCS study (Cialone et al. 2015). Manning's  $n$  was set to the NACCS values, except for the areas in the higher-resolution area of the ADCIRC mesh, where the Manning's  $n$  values were reset to those used in a previous study (Orescanin et al. 2016). Additional ADCIRC model input parameters include a nonlinear bottom friction with finite amplitude terms and a lower limit of bottom friction (FFACTOR) of 0.003, nonlinear advection terms in space and time, a 2.0-day ramp period using the hyperbolic tangent ramping function, a wetting and drying threshold depth of 0.10 m, and a minimum wetting velocity of 0.10 m/s.

### Model Coupling

To simulate surge levels, wind waves, currents, and the interactions among them, ADCIRC and STWAVE were two-way coupled in water level and wave-radiation stresses using the Coastal Storm

Modeling System (CSTORM-MS) coupler (Massey et al. 2011b). This coupling enables ADCIRC to pass water levels and current velocities to STWAVE and to receive wave-radiation-stress gradients during run time at every STWAVE snap (every 30 min). With this coupling, wind blowing over inundated regions during high surge events will generate waves. Both ADCIRC and STWAVE were run in their parallel computing modes by partitioning the domain to utilize high-performance computing resources at the Hamming cluster at the Naval Postgraduate School and the Topaz SGI system at the United States Army Corps of Engineers High Performance Computing Center. The three models compared here are the (1) NACCS coarse resolution coupled model (NACCS); (2) the high-resolution ADCIRC-only model (KB-ADCIRC); and (3) the high-resolution coupled model (KB-CSTORM).

## Results and Discussion

### Observational Data

To assess the accuracy of the models, comparisons were made with observations during Hurricane Irene in Katama Bay. Water elevation was estimated with bottom-mounted pressure sensors (sampled at 2 Hz) along the north–south axis of the bay (circles, Stations 01–03, Fig. 1). Station 01, the northernmost station, is near the transition from the bay to Vineyard Sound through Edgartown Channel. Station 02 is the farthest from any land boundary interaction and characterizes Katama Bay. Station 03 is close to Katama Inlet, near the transition from the Atlantic Ocean to Katama Bay. More details of the observations can be found in Orescanin et al. (2014). Model results also were output at 10 additional locations

within the bay, as well as on the ebb shoal (Station 04) to simulate conditions outside of the bay.

## Model Evaluation

### Error Statistics

As is seen in many storm surge modeling efforts (Orton et al. 2012; Sun et al. 2013), modeled water-elevation levels were less than observed, with the maximum under prediction during peak surge [Figs. 2(c and d)]. Water level is predicted more accurately by the models that use high-spatial-resolution meshes (KB-ADCIRC and KB-CSTORM) than by the lower-resolution NACCS model (Fig. 2 and Table 1). The high-resolution model (KB-ADCIRC and KB-CSTORM) predictions of the timing of the peak storm surge are more accurate than the NACCS predictions, which tend to lag the observed peak surge (Fig. 2). The coupled KB-CSTORM has somewhat lower errors than KB-ADCIRC at the center [Fig. 2(d), Station 02] and southern side [Fig. 2(e), Station 03] of the bay, particularly during the 12-h period of peak storm surge (Fig. 2 and Table 1, Column 4). The 12-h period was selected to represent the shortest duration of peak storm and provides an end-member estimate of the reduction of error (the RMSE will be bounded by the typical conditions and peak storm duration). The reduction in error percentage by coupling with the wave model is small during calm conditions, but increases during the peak surge

**Table 1.** Root-mean square error between modeled and observed water levels for the total duration time series (Column 3) and for the 12-h window centered on the time of the peak surge (storm duration, Column 4)

Station	Model	Storm duration	
		Total timeseries RMSE (m)	RMSE (m)
01	NACCS	0.18	0.27
	KB-ADCIRC	0.18	0.30
	KB-CSTORM	0.17	0.24
02	NACCS	0.16	0.31
	KB-ADCIRC	0.15	0.28
	KB-CSTORM	0.13	0.19
03	NACCS	0.22	0.33
	KB-ADCIRC	0.08	0.16
	KB-CSTORM	0.10	0.19
Average	NACCS	0.19	0.30
	KB-ADCIRC	0.14	0.25
	KB-CSTORM	0.13	0.21

period, suggesting that both bottom topography and waves are important to modeling hydrodynamics near inlets.

## Spatial Comparisons

**Resolution Effects.** Increasing spatial resolution leads to more accurate modeled values. However, another explanation for the difference in accuracy between the NACCS and the high-resolution runs is that during NACCS mesh development, the southern shoreline [Norton Point, Figs. 1 and 3(a)] is made into a hard no-normal-flow boundary. The result is that NACCS does not allow flow through Katama Inlet nor the overtopping of the beach that occurred during Hurricane Irene. The lack of inlet currents and of overtopping can explain many of the flow-pattern differences between the high-resolution models and the NACCS. The NACCS does not allow Atlantic water to enter Katama Bay from the south, and thus the simulated circulation [Fig. 10(a), NACCS] and water levels (Fig. 2, NACCS) in the bay are owing to wind stress and to water entering or exiting through Edgartown Channel to the north, in contrast with the high-resolution models [Figs. 5 and 6(b), KB-CSTORM] and with the observations during peak surge conditions. In addition, the high-resolution models indicate a narrow coastal jet with magnitudes over 2.0 m/s along the southern coast that is not apparent in the lower-resolution simulations. Currents also are amplified within the Bay and Edgartown Channel relative to those simulated with NACCS [compare Figs. 10(b and c) with Fig. 10(a)], indicating a net northward circulation, consistent with previous results (Orescanin et al. 2014). Comparing the effects of resolution and waves on velocity during peak surge suggests not only increased northward flow through Katama Bay for KB-ADCIRC [Fig. 10(b)] and KB-CSTORM [Fig. 10(c)], but also an enhanced coastal current during KB-CSTORM compared with KB-ADCIRC, suggesting the influence of waves is to concentrate flows along the coast.

During the peak surge, the NACCS model tends to have higher water levels on the southern shoreline than either of the high-resolution models [Fig. 2(f)]. The approximately 0.3-m increase in NACCS modeled water level suggests that the high-resolution bathymetry that includes the relatively small Katama Inlet may have a relatively large effect on shoreline water levels. In addition, the predicted increase in surge on the southern shore simulated by the low-resolution model with no inlet suggests a possibility of enhanced overtopping along Norton Point when the inlet is closed, consistent with the observation that Katama Inlet opens during extreme surge events.

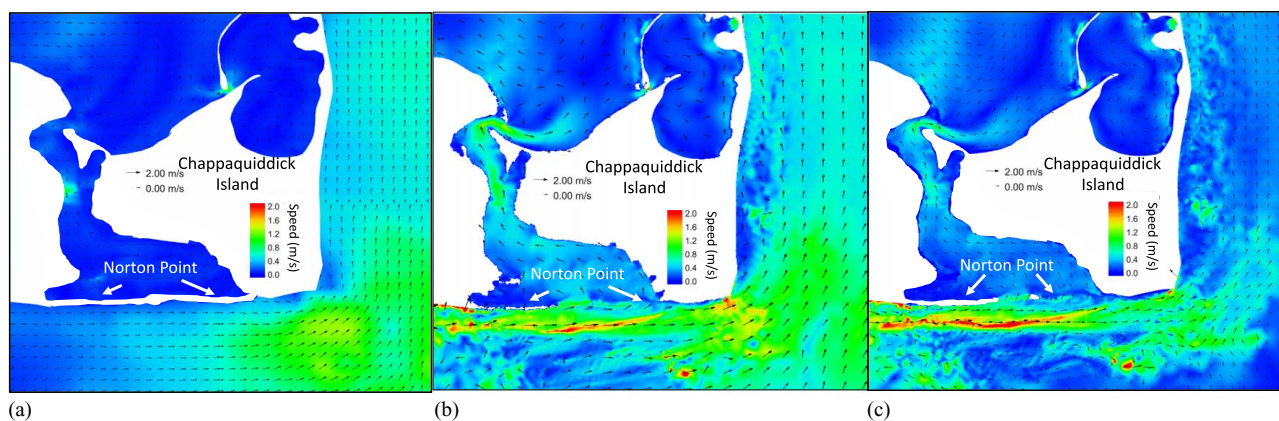


**Fig. 10.** Contours of current speed (color bars are inset) and vectors (point in the direction of the current with length proportional to speed, scale left of and above the color bars) for (a) NACCS; (b) KB-ADCIRC; and (c) KB-CSTORM during peak surge. Norton Point is indicated by arrows.



**Coupling Effects.** Error statistics show that the coupling of STWAVE and ADCIRC in KB-CSTORM improves prediction performance compared with using ADCIRC alone (KB-ADCIRC), especially on the southern shore and within Katama Bay. For example, during the peak storm surge, KB-CSTORM includes wave-driven setup and predicts significantly (up to 0.3 m) higher water elevations in the southern part of Katama Bay and in the surf zone directly to the south than are predicted by KB-ADCIRC (Fig. 11). In addition, the overall higher water levels within Katama Bay predicted by KB-CSTORM during peak surge indicates waves are contributing to an overall elevation change within the bay, consistent with previous results for single-inlet systems (Malhadas et al. 2009; Olabarrieta et al. 2011). Although the more common moderate wave forcing

may not increase the bay water levels (Orescanin et al. 2014), during surge events not all wave-driven momentum flux entering the bay through Katama Inlet can be radiated out of the bay through Edgartown Channel, resulting in an overall bay setup that is common in single-inlet systems.

Currents simulated by the higher-resolution KB-ADCIRC and KB-CSTORM models have tidal fluctuations throughout the Bay in contrast to the weaker (and nontidal) velocities predicted by the coarser NACCS model (not shown). KB-ADCIRC and KB-CSTORM velocities are nearly identical during calm wave conditions, but deviate during Irene, with KB-CSTORM predicting a reduced ebb current (to zero flow) during the peak of the storm, consistent with the breaking-wave-driven currents observed at Katama Inlet (Orescanin et al. 2014).

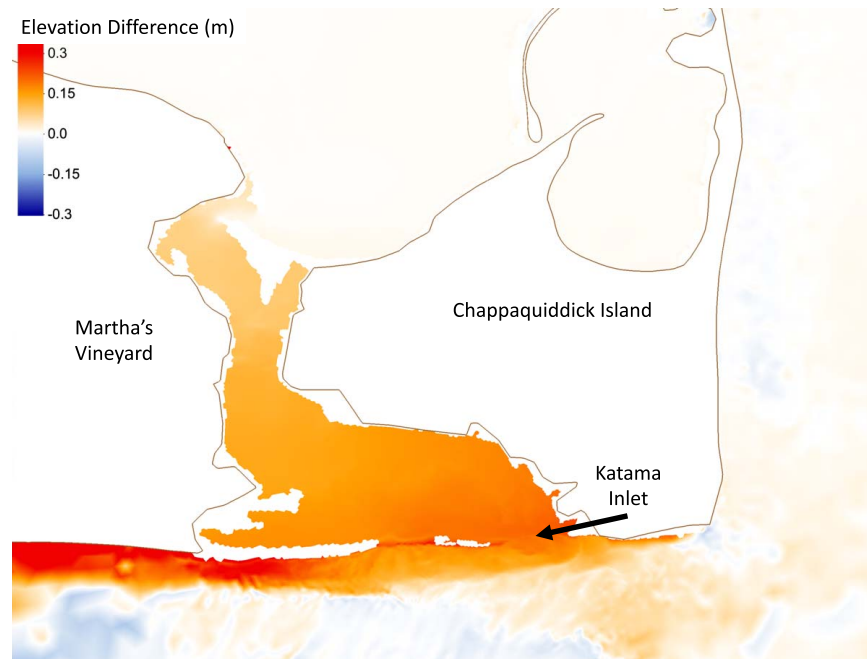


**Fig. 11.** Contours (color bar in the upper left) of water elevation difference between KB-CSTORM and KB-ADCIRC model runs during peak storm surge.

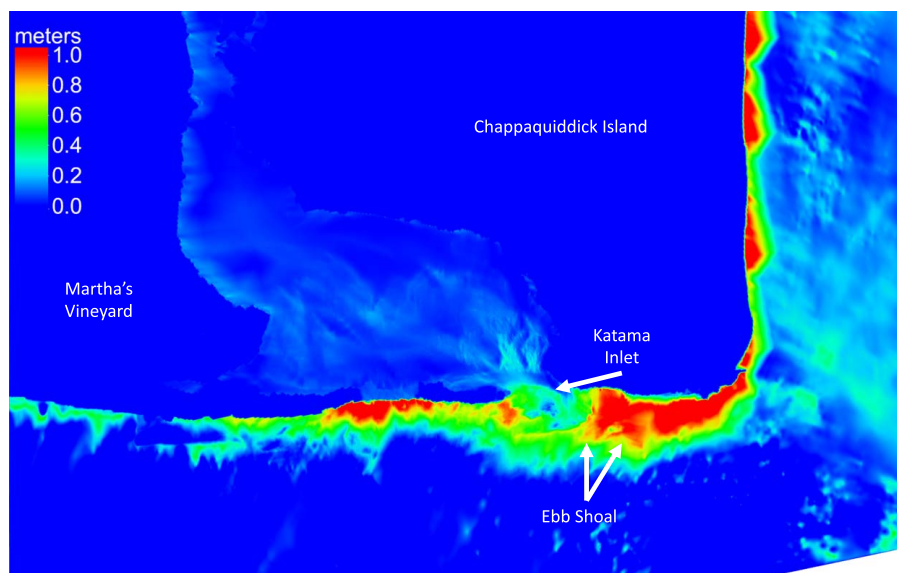


**Fig. 12.** Contours (color bar in the upper left) of wave height difference between KB-CSTORM and NACCS model runs during peak storm surge.

**Table 2.** Error reduction relative to the low-spatial resolution NACCS results

Model	Total timeseries error reduction (%)	Storm duration error reduction (%)
KB-ADCIRC	26.3	16.7
KB-CSTORM	31.6	30.0

Note: Reduction is defined as  $(RMSE_{NACCS} - RMSE_{KBXX}) / RMSE_{NACCS} \times 100\%$  from the average values (bottom rows in Table 1).

At some locations, KB-CSTORM predicts much larger ( $>1$  m) significant wave heights than NACCS predicts, especially near the shore (Fig. 12). Both models predicted approximately 0.5-m wave height in the center of the bay (Fig. 1, Station 02) during the peak of the storm, in contrast to the observed approximately 0.2-m wave height (not shown). On the ebb shoal (Fig. 1, Station 04, just offshore off the mouth of Katama Inlet) NACCS predicts much smaller wave heights than KB-CSTORM predicts (Fig. 12). There were no observations on the ebb shoal, but comparisons of model predictions with observations of waves in 12-m depth, a few km south of the ebb shoal (Martha's Vineyard Coastal Observatory, <https://www.whoi.edu/mvco>, not shown) suggest the modeled wave heights are similar to those observed (up to 5-m significant wave height) before and after the peak of the storm (the MVCO sensor did not operate for a few hours during the peak of the storm). The KB-CSTORM model predicts approximately 3-m wave heights on the ebb shoal during the peak of the storm, whereas the NACCS model predicts 1.5-m wave heights. The underprediction of wave heights by NACCS (near the ebb shoal, Fig. 12) may be related to the low-resolution bathymetry or to the lack of two-way coupling with the wave model (Table 2).

## Conclusions

Comparisons of simulations with observations in the Katama Bay system prior to and during Hurricane Irene indicate that the coupling of wave (STWAVE) with circulation (ADCIRC) models in addition to using high-resolution bathymetry (KB-CSTORM) results in better predictions of wave heights and water levels during Hurricane Irene than predicted with the lower resolution (KB-NACCS) or with the high resolution, no wave (KB-ADCIRC) models. These results suggest that both high-spatial resolution of small ( $<400$  m) tidal inlets and wave coupling are required for accurate surge prediction. During the peak surge of Hurricane Irene, errors in water level elevations were 30% lower using KB-CSTORM than using NACCS. The improved model predictions primarily are owing to resolving the inlet and nearby shorelines in the KB-CSTORM model, whereas the low-spatial resolution NACCS does not include the inlet nor does it allow overwash of the sand barrier separating Katama Bay from the ocean. An artifact of the low-resolution bathymetry is higher water levels and smaller currents along the shoreline than predicted by KB-CSTORM, which could lead to inaccurate predictions of sediment transport and morphological change.

Prior studies during moderate wave conditions show that water driven into Katama Bay by breaking-wave-induced momentum flux leaves the bay through Edgartown Channel, and thus bay water levels do not increase. In contrast, during extreme events (e.g., Hurricane Irene), model simulations suggest the flux through Edgartown Channel is insufficient to balance the breaking-wave-induced increased flows into Katama Bay through Katama Inlet, resulting in an increased water elevation in the bay. The increased water levels within the bay during storms can result in relatively large waves that could erode the banks and flood surrounding marshes.

## Data Availability Statement

NDBC data can be found at: <https://www.ndbc.noaa.gov>. Observational data and model outputs from ADCIRC and STWAVE that support the findings of this study are available from the corresponding author upon reasonable request.

## Acknowledgments

We thank Levi Gorrell and the PVLAB field crew for deploying, maintaining, and recovering sensors in sometimes less-than-ideal conditions. Thanks to MVCO for wave height and wind velocity time series. Funding was provided by a Vannevar Bush Faculty Fellowship [OUSD(R&E)], Sea Grant, the National Science Foundation (NSF), and Office of Naval Research.

## References

- Bennett, V. C. C., R. P. Mulligan, and C. J. Hapke. 2018. "A numerical model investigation of the impacts of Hurricane Sandy on water level variability in Great South Bay, New York." *Cont. Shelf Res.* 161: 1–11. <https://doi.org/10.1016/j.csr.2018.04.003>.
- Bertin, X., A. B. Fortunato, and A. Oliveira. 2009. "A modeling-based analysis of processes driving wave-dominated inlets." *Cont. Shelf Res.* 29 (5–6): 819–834. <https://doi.org/10.1016/j.csr.2008.12.019>.
- Blain, C. A., J. J. Westerink, and R. A. Luettich Jr. 1994. "The influence of domain size on the response characteristics of a hurricane storm surge model." *J. Geophys. Res.* 99 (C9): 18467. <https://doi.org/10.1029/94JC01348>.
- Blake, E. S., E. N. Rappaport, J. D. Jarrell, and C. W. Landsea. 2007. *The deadliest, costliest and most intense United States hurricanes from 1851 to 2004 (and other frequently requested hurricane facts)*. Technical Memorandum NWS-TPC-5. Washington, DC: NOAA.
- Bryant, M. A., and R. E. Jensen. 2017. "Application of the nearshore wave model STWAVE to the North Atlantic coast comprehensive study." *J. Waterway, Port, Coastal, Ocean Eng.* 143 (5): 04017026. [https://doi.org/10.1061/\(ASCE\)WW.1943-5460.0000412](https://doi.org/10.1061/(ASCE)WW.1943-5460.0000412).
- Chen, C., et al. 2013. *An unstructured-grid, finite-volume community ocean model FVCOM user manual*. 3rd ed. SMASST/UMASSD Technical Rep. No. 13-0701. New Bedford, MA: Univ. of Massachusetts-Dartmouth.
- Cialone, M. A., A. S. Grzegorzewski, D. J. Mark, M. A. Bryant, and T. C. Massey. 2017. "Coastal-storm model development and water-level validation for the North Atlantic coast comprehensive study." *J. Waterway, Port, Coastal, Ocean Eng.* 143 (5): 04017031. [https://doi.org/10.1061/\(ASCE\)WW.1943-5460.0000408](https://doi.org/10.1061/(ASCE)WW.1943-5460.0000408).
- Cialone, M. A., T. C. Massey, M. E. Anderson, A. S. Grzegorzewski, R. E. Jensen, A. Cialone, D. J. Mark, K. C. Pevey, B. L. Gunkel, and T. O. McAlpin. 2015. *North Atlantic Coast comprehensive study (NACCS) coastal storm model simulations: Waves and water levels*. ERDC/CHL TR-15-14. Vicksburg, MS: U.S. Army Engineering Research and Development Center.
- Dietrich, J., S. Tanaka, J. Westerink, C. Dawson, R. Luettich Jr., M. Zijlema, L. Holthuijsen, J. Smith, L. Westerink, and H. Westerink. 2012. "Performance of the unstructured-mesh, SWAN + ADCIRC model in computing hurricane waves and surge." *J. Sci. Comput.* 52 (2): 468–497. <https://doi.org/10.1007/s10915-011-9555-6>.
- Dodet, G., X. Bertin, N. Bruneau, A. B. Fortunato, A. Nahon, and A. Roland. 2013. "Wave-current interactions in a wave-dominated tidal inlet." *J. Geophys. Res.: Oceans* 118 (3): 1587–1605. <https://doi.org/10.1002/jgrc.20146>.
- Gonçalves, M., E. Rusu, and C. Guedes Soares. 2015. "Evaluation of two spectral wave models in coastal areas." *J. Coastal Res.* 300: 326–339. <https://doi.org/10.2112/JCOASTRES-D-12-00226.1>.
- Hopkins, J., S. Elgar, and B. Raubenheimer. 2016. "Observations and model simulations of wave-current interaction on the inner shelf."

- J. Geophys. Res.: Oceans* 121 (1): 198–208. <https://doi.org/10.1002/2015JC010788>.
- Hopkins, J., S. Elgar, and B. Raubenheimer. 2017. “Flow separation effects on shoreline sediment transport.” *Coastal Eng.* 125: 23–27. <https://doi.org/10.1016/j.coastaleng.2017.04.007>.
- Jensen, R., A. Cialone, J. Smith, M. Bryant, and T. Hesser. 2016. “Regional wave modeling and evaluation for the North Atlantic Coast comprehensive study.” *J. Waterway, Port, Coastal, Ocean Eng.* 143 (2): B4016001. [https://doi.org/10.1061/\(ASCE\)WW.1943-5460.0000342](https://doi.org/10.1061/(ASCE)WW.1943-5460.0000342).
- Kang, X., and M. Xia. 2020. “The study of the hurricane-induced storm surge and bay-ocean exchange using a nesting model.” *Estuaries Coasts* 1–15. <https://doi.org/10.1007/s12237-020-00695-3>.
- Kerr, P. C., R. C. Martyr, A. S. Donahue, M. E. Hope, J. J. Westerink, R. A. Luettich, A. B. Kennedy, J. C. Dietrich, C. Dawson, and H. J. Westerink. 2013. “U.S. IOOS coastal and ocean modeling testbed: Evaluation of tide, wave, and hurricane surge response sensitivities to mesh resolution and friction in the Gulf of Mexico.” *J. Geophys. Res.: Oceans* 118 (9): 4633–4661. <https://doi.org/10.1002/jgrc.20305>.
- Komen, G. J., L. Cavaleri, M. Donelan, K. Hasselmann, S. Hasselmann, and P. A. E. M. Janssen. 1994. *Dynamics and modeling of ocean waves*. Cambridge: Cambridge University Press.
- Kumar, N., G. Voulgaris, and J. C. Warner. 2011. “Implementation and modification of a three-dimensional radiation stress formulation for surf zone and rip-current applications.” *Coastal Eng.* 58 (12): 1097–1117. <https://doi.org/10.1016/j.coastaleng.2011.06.009>.
- Lawler, S., J. Haddad, and C. M. Ferreira. 2016. “Sensitivity considerations and the impact of spatial scaling for storm surge modeling in wetlands of the Mid-Atlantic region.” *Ocean Coastal Manage.* 134: 226–238. <https://doi.org/10.1016/j.ocecoaman.2016.10.008>.
- Luettich, R. A., Jr., J. J. Westerink, and N. W. Scheffner. 1992. *ADCIRC: An advanced three-dimensional circulation model for shelves, coasts, and estuaries*. Technical Rep. No. DRP-92-6. Vicksburg, MS: U.S. Army Engineer Research and Development Center.
- Malhadas, M. S., P. C. Leitao, A. Silva, and R. Neves. 2009. “Effect of coastal waves on sea level in Obidos Lagoon, Portugal.” *Cont. Shelf Res.* 29 (9): 1240–1250. <https://doi.org/10.1016/j.csr.2009.02.007>.
- Mao, M., and M. Xia. 2018. “Wave–current dynamics and interactions near the two inlets of a shallow lagoon–inlet–coastal ocean system under hurricane conditions.” *Ocean Modell.* 129: 124–144. <https://doi.org/10.1016/j.oceomod.2018.08.002>.
- Massey, T. C., M. E. Anderson, J. M. Smith, J. Gomez, and R. Jones. 2011a. *STWAVE: Steady-state spectral wave model user’s manual for STWAVE, version 6.0*. ERDC/CHL SR–11–1. Vicksburg, MS: U.S. Army Engineer Research and Development Center.
- Massey, T. C., T. V. Wamsley, and M. A. Cialone. 2011b. “Coastal storm modeling—System integration.” In *Proc., 2011 Solutions to Coastal Disasters Conf.*, 99–108.
- Neumann, J., K. Emanuel, S. Ravela, L. Ludwig, P. Kirshen, K. Bosma, and J. Martinich. 2015. “Joint effects of storm surge and sea-level rise on US coasts: New economic estimates of impacts, adaptation, and benefits of mitigation policy.” *Clim. Change* 129 (1–2): 337–349. <https://doi.org/10.1007/s10584-014-1304-z>.
- Olabarrieta, M., J. C. Warner, and N. Kumar. 2011. “Wave–current interaction in Willapa Bay.” *J. Geophys. Res.* 116: C12014. <https://doi.org/10.1029/2011JC007387>.
- Orescanin, M., S. Elgar, and B. Raubenheimer. 2016. “Changes in bay circulation in an evolving multiple inlet system.” *Cont. Shelf Res.* 124: 13–22. <https://doi.org/10.1016/j.csr.2016.05.005>.
- Orescanin, M., B. Raubenheimer, and S. Elgar. 2014. “Observations of wave effects on inlet circulation.” *Cont. Shelf Res.* 82: 37–42. <https://doi.org/10.1016/j.csr.2014.04.010>.
- Orton, P., N. Georgas, A. Blumberg, and J. Pullen. 2012. “Detailed modeling of recent severe storm tides in estuaries of the New York City region.” *J. Geophys. Res.: Oceans* 117: C09030. <https://doi.org/10.1029/2012JC008220>.
- OWI (Oceanweather, Inc.). 2015. *Development of wind and pressure forcing for the North Atlantic Coast Comprehensive Study (NACCS)*. Stamford, CT: U.S. Army Engineer, Engineer Research and Development Center.
- Smith, J. M., and S. J. Smith. 2002. *Grid nesting with STWAVE*. ERDC/CHL CHETN I-66. Vicksburg, MS: U.S. Army Engineer Research and Development Center.
- Sun, Y., C. Chen, R. C. Beardsley, Q. Xu, J. Qi, and H. Lin. 2013. “Impact of current-wave interaction on storm surge simulation: A case study for Hurricane Bob.” *J. Geophys. Res.: Oceans* 118 (5): 2685–2701. <https://doi.org/10.1002/jgrc.20207>.
- SWAN Team. 2017. *Scientific and technical documentation for SWAN cycle III, version 41.20*. Delft, Netherlands: Delft Univ. of Technology.
- Tolman, H. L. 2014. *User manual and system documentation of WaveWatch III, version 4.18*. Technical Note. MMAB Contribution No. 316. Washington, DC: U.S. Department of Commerce.
- Westerink, J. J., R. A. Luettich, A. M. Baptists, N. W. Scheffner, and P. Farrar. 1992. “Tide and storm surge predictions using finite element model.” *J. Hydraul. Eng.* 118 (10): 1373–1390. [https://doi.org/10.1061/\(ASCE\)0733-9429\(1992\)118:10\(1373\)](https://doi.org/10.1061/(ASCE)0733-9429(1992)118:10(1373)).
- Yin, J., N. Lin, and D. Yu. 2016. “Coupled modeling of storm surge and coastal inundation: A case study in New York City during Hurricane Sandy.” *Water Resour. Res.* 52 (11): 8685–8699. <https://doi.org/10.1002/2016WR019102>.